LES of Single Droplet and Liquid Jet Primary Break-up Using a Coupled Level Set/Volume of Fluid Method

F. Xiao*, M. Dianat, and J. J. McGuirk
Department of Aeronautical and Automotive Engineering, Loughborough University, UK
F.Xiao2@lboro.ac.uk, M.Dianat@lboro.ac.uk, and J.J.McGuirk@lboro.ac.uk

Abstract

Numerical modelling of primary break-up of a liquid jet under the influence of strong aerodynamic and turbulence effects is very challenging, especially for high liquid/gas density ratio O (1000). A robust algorithm for Large Eddy Simulation (LES) of two-phase flows is presented here. A Coupled Level Set and Volume of Fluid (CLSVOF) technique is applied as the interface-tracking method in order to combine the advantages of LS and VOF methods. The governing equations are discretised by introducing an extrapolated liquid velocity to minimise the interface momentum error. Since experimental studies on break-up of a single liquid drop in uniform gas flow are well documented, this test case is first used to validate the developed two-phase flow LES method. It is shown that the predicted drop break-up agrees quantitatively well with experiments for different Weber numbers. The solver is then applied to simulate primary break-up of liquid jets, which are more relevant to industrial applications. By simulating single round water jet atomisation in high-speed coaxial air flow (Charalampous et al. [19]), it is found that the predicted liquid core break-up lengths at different air/liquid velocities agree closely with measured data, but only when appropriate turbulent inflow conditions are specified.

Introduction

An accurate method for prediction of liquid jet atomisation is of utmost significance in many industrial applications, with the engineering driver of prime interest in the present work being the aeroengine gas turbine fuel injector. Substantial experimental and computational research has been carried out to understand the first stage of the atomisation process — primary break-up. However, numerical modelling of primary break-up of a liquid jet is very challenging, especially for the conditions relevant to air-blast atomisation in gas turbine combustors — highly turbulent flows, strong aerodynamic forces, and high liquid/gas density ratio. Simulations can become unstable due to errors in dealing with discontinuous conditions across the interface. As a consequence, many published numerical simulations to date have been limited to a liquid/gas density ratio no more than ~100 (see [1] – [4]). Since the majority of liquid jet atomisation experiments are carried out at atmospheric pressure with high density liquids, quantitative comparison between numerical modelling and experiment is quite rare. The simulation reported in [5] applied the algorithm proposed in [6] to a liquid (Jet-A) jet in air cross-flow and hence had a high (650) density ratio. Adaptive Mesh Refinement and the removal of under-resolved small liquid structures were necessary since the only experimental data available was far downstream; in spite of the advanced modelling, agreement with measurements was relatively poor. The current research is focused specifically on the early stage of primary break-up and its objectives are: (i) to develop a Large Eddy Simulation (LES) methodology for simulating the atomisation of turbulent liquid jets in highly turbulent gas flow at a high density ratio, and (ii) to validate the method against experimental data for both single droplet break-up in a uniform air flow and liquid jet atomisation in a coaxial, co-annular air flow. A Coupled Level Set and Volume of Fluid (CLSVOF) technique is adopted as the interface-tracking method, since it seems to be the optimum approach simultaneously to conserve liquid mass and provide superior resolution of the interface geometry, combining the advantages of VOF and LS methods. In the current approach to two-phase flow modelling, a single set of governing equations is solved for both liquid and gas phases. Since the density is discontinuous across the interface, momentum is also discontinuous. Thus, an appropriate numerical scheme is required to treat such discontinuities when discretising the momentum equations. Sussman et al. [6] proposed a method to use an extrapolated liquid velocity. Such an approach has been used in modified form in the current study. A different way of extrapolating liquid velocity is implemented, and a liquid divergence-free step is added to obtain higher robustness and accuracy. In contrast with the method of [6], where a complex algorithm is applied for the discretisation of the momentum equations using both staggered and co-located velocity components, a simple scheme using only staggered velocities is proposed. With these improvements, appropriate boundary conditions are imposed at the two-phase interface, leading to stable solutions even for high liquid/gas density ratio O(1000). The surface tension at the interface is treated via a ghost fluid approach [7] by incorporating the pressure jump into the discretisation of the pressure gradient. In the following sections, the

* Corresponding author: F.Xiao2@lboro.ac.uk

numerical method for two-phase flow modelling is first described. The developed algorithm is then validated using two test cases: single drop break-up in a uniform flow, and liquid jet atomisation in a turbulent coaxial, co-annular gas flow. All simulations have been carried out with water (liquid) and air (gas) at atmospheric pressure, resulting in a high density ratio of 830.

Governing Equations

Coupled Level Set and Volume of Fluid Interface Capture Method

The VOF function *F* is defined as the volume fraction occupied by the liquid. The fully (temporally and spatially) resolved evolution of *F* is governed by:

$$\frac{\partial F}{\partial t}+U_k\frac{\partial F}{\partial x_k}=0$$

The LS function ϕ is interpreted as the signed distance from the interface satisfying $|\nabla\phi|=1$. The interface is defined by $\phi=0$, with $\phi>0$ representing liquid and $\phi<0$ representing air. ϕ is evolved (in a fully resolved sense) by solving the simple advection equation:

$$\frac{\partial \phi}{\partial t}+U_k\frac{\partial \phi}{\partial x_k}=0$$

To maintain a signed-distance property, a re-initialisation equation is solved, where τ represents fictitious time:

$$\frac{\partial \phi}{\partial \tau}=sign(\phi)\left(1-\sqrt{\frac{\partial \phi}{\partial x_i}.\frac{\partial \phi}{\partial x_i}}\right)$$

this is solved until steady state is reached near the interface. Coupling of ϕ and F equations is described below.

Two-Phase Flow Transport Equations

In the current study of two-phase flow modelling, both liquid and gas are assumed to be incompressible and immiscible. The continuity equation is then the same as that for single-phase flows:

$$\frac{\partial U_k}{\partial x_k}=0$$

The momentum equations must allow for fluid property discontinuity and surface tension at the interface:

$$\frac{\partial U_k}{\partial t}+\frac{\partial (U_lU_k)}{\partial x_l}=-\frac{1}{\rho}\frac{\partial P}{\partial x_k}+\frac{1}{\rho}\frac{\partial \tau_{kl}}{\partial x_l}+g_k+\frac{1}{\rho}F_k^{ST}$$

$$\tau_{kl}=\mu(\frac{\partial U_k}{\partial x_l}+\frac{\partial U_l}{\partial x_k}),\qquad \rho=\rho_G+(\rho_L-\rho_G)H(\phi),\ \ \mu=\mu_G+(\mu_L-\mu_G)H(\phi)$$

Where g_k is gravitational acceleration and $H(\phi)$ is the Heaviside function. The surface tension force F_k^{ST} is:

$$F_k^{ST}=\sigma\kappa\frac{\partial H}{\partial x_k}\qquad \kappa=\frac{\partial n_k}{\partial x_k}=\frac{\partial}{\partial x_k}\left(-\frac{1}{\sqrt{\frac{\partial \phi}{\partial x_i}.\frac{\partial \phi}{\partial x_i}}}\frac{\partial \phi}{\partial x_k}\right)$$

σ is surface tension coefficient, κ is curvature and n_k is the interface normal vector (pointing from liquid to gas).

Large Eddy Simulation (LES) Formulation

The philosophy for the current approach to two-phase LES is as follows: the usual spatially filtered LES formulation is employed in the single-phase flow regions with proper boundary conditions imposed on the interface for both phases (detailed in the following sections). The continuity equation becomes:

$$\frac{\partial \overline{U_k}}{\partial x_k}=0$$

where an overbar represents spatial filtering. The residual or sub-grid-scale (SGS) stress tensor which appears in the resolved scale filtered momentum equations is modelled by a simple Smagorinsky eddy viscosity approach (Δ represents the filter width, taken as the cube root of the local cell volume); the SGS term arising from the surface tension term filtering is neglected (see comment below on the spatial resolution of the interface):

$$\frac{\partial \overline{U_k}}{\partial t}+\frac{\partial (\overline{U_l}\overline{U_k})}{\partial x_l}=-\frac{1}{\rho}\frac{\partial \overline{P}}{\partial x_k}+\frac{1}{\rho}\frac{\partial\left(\overline{\tau}_{kl}+\overline{\tau}_{kl}^{r}\right)}{\partial x_l}+g_k+\frac{1}{\rho}\overline{F}_k^{ST}$$

$$\overline{\tau}_{kl}=2\mu\overline{S}_{kl},\quad \overline{\tau}_{kl}^{r}=2\mu_{SGS}\overline{S}_{kl},\quad \overline{S}_{kl}=\frac{1}{2}\left(\frac{\partial \overline{U}_k}{\partial x_l}+\frac{\partial \overline{U}_l}{\partial x_k}\right),\quad \mu_{SGS}=\rho(C_S\Delta)^2S\quad S=(2\overline{S}_{kl}\overline{S}_{kl})^{\frac{1}{2}}$$

$$\rho=\rho_G+(\rho_L-\rho_G)H(\overline{\phi}),\ \ \mu=\mu_G+(\mu_L-\mu_G)H(\overline{\phi})$$

Note that the same momentum equations are solved within single phase regions of the flow as well as in the zone containing the interface. Since it is desired to maintain the implications of a sharp interface, fluid density and viscosity are in the present approach not considered as spatially filtered quantities, but are set to be the properties of liquid or gas depending on the local value of the resolved Level Set $\overline{\phi}$. The VOF function is discontinuous across the interface; spatial filtering will regularise *F* to a continuous function and smear the interface - some element of which is, however, inevitable in any discretised methodology. The instantaneous VOF equation written in terms of resolved scale and SGS velocity components (u'_k) is:

$$\frac{\partial F}{\partial t}+U_k\frac{\partial F}{\partial x_k}=\frac{\partial F}{\partial t}+\left(\overline{U}_k+u'_k\right)\frac{\partial F}{\partial x_k}=0$$

Whilst modelling approaches for reconstructing the SGS velocity have been proposed [8], these have not yet developed into a generally demonstrated and workable method. Equally, the liquid volume flux is dominated by the filtered velocity, and the contribution of the SGS velocity is small. Thus the SGS term in the VOF equation is neglected, resulting in the following transport equation solved for resolved VOF function $\overline{F}$:

$$\frac{\partial \overline{F}}{\partial t}+\overline{U}_k\frac{\partial \overline{F}}{\partial x_k}=0 \qquad \frac{\partial \overline{\phi}}{\partial t}+\overline{U}_k\frac{\partial \overline{\phi}}{\partial x_k}=0$$

As indicated above, an analogous treatment is adopted for the transport equation for resolved Level Set $\overline{\phi}$; as a consequence, the resolved interface geometry cannot track distortions due to the smallest eddies, and this is the reason no SGS component of the surface tension force was retained. The resolved surface tension term becomes:

$$\overline{F}_k^{ST}=\sigma\overline{\kappa}\frac{\partial H}{\partial x_k} \qquad \overline{\kappa}=\frac{\partial \overline{n}_k}{\partial x_k}=\frac{\partial}{\partial x_k}\left(-\frac{1}{\sqrt{\frac{\partial\overline{\phi}}{\partial x_i}\cdot\frac{\partial\overline{\phi}}{\partial x_i}}}\frac{\partial\overline{\phi}}{\partial x_k}\right)$$

Thus, in the present work the LES formulation is similar to that referred to in [9] as "quasi-DNS/LES", i.e. an under-resolved DNS of the interface combined with an LES of the single phase regions of the flow; the treatment of fluid density and viscosity is, however, different.

Numerical Method

Temporal Discretisation

The forward Euler projection method is used for temporal discretisation of the two-phase governing equations. First, an intermediate velocity is computed from convection, diffusion and gravitational terms (NB surface tension is treated as part of the pressure term using the ghost-fluid approach to be described below):

$$\frac{\overline{U}_k^*-\overline{U}_k^n}{\delta t}=-\frac{\partial}{\partial x_l}\left(\overline{U}_l^n\overline{U}_k^n\right)+\frac{1}{\rho}\frac{\partial}{\partial x_l}\left(\overline{\tau}_{kl}^n+\overline{\tau}_{kl}^{r,n}\right)+g_k$$

The intermediate velocity is updated using a pressure gradient term to obtain the velocity at time step $n+1$:

$$\frac{\overline{U}_k^{n+1}-\overline{U}_k^*}{\delta t}=-\frac{1}{\rho}\frac{\partial\overline{P}^{n+1}}{\partial x_k}$$

Since the velocity field at time step $n+1$ should satisfy continuity, a pressure Poisson equation is derived by taking the divergence of the above equation, and solved to obtain the pressure field to be used in the update step:

$$\frac{\partial}{\partial x_k}\left(\frac{1}{\rho}\frac{\partial\overline{P}^{n+1}}{\partial x_k}\right)=\frac{1}{\delta t}\frac{\partial\overline{U}_k^*}{\partial x_k}$$

Grid and Variable Arrangement

To illustrate particular details, discretisation of the u (x-momentum) equation is illustrated here on a 2D grid. The mesh and variable storage arrangement used are shown in Fig 1. Variables are arranged in a staggered manner: ρ, μ, pressure, LS and VOF are located at cell centres; velocity components at corresponding faces.

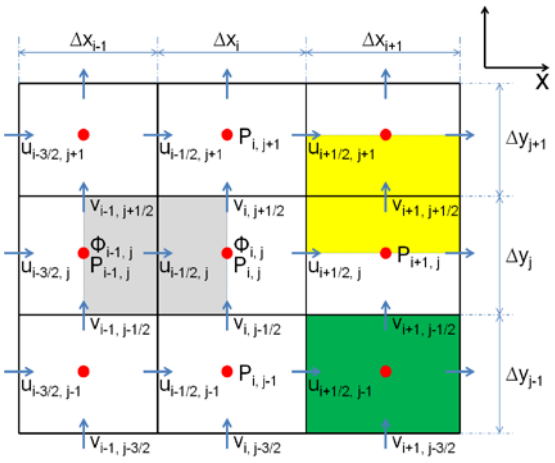

Fig. 1 Grid/staggered variable arrangement

LS and VOF Spatial Discretisation and Coupling

In solving the F equation a piecewise linear interface calculation (PLIC) method is used to reconstruct the interface (details below). Based on the computed interface, the liquid volume flux advected through each face of the cell is calculated geometrically to minimise numerical diffusion of the discontinuous VOF function. An operator split method is used, following [10], due to its straightforward implementation. It is often asserted in the litera-

ture that high-order spatial discretisation methods (e.g. 5th-order WENO) are necessary for evolving LS in pure level set methods to minimise mass conservation errors. The 5th-order WENO method has also been used for LS advection/re-initialisation in some CLSVOF methods [11]. However, WENO schemes [12] for LS advection and re-initialisation have primarily been applied only on uniform Cartesian meshes. A further drawback of WENO is its high computational cost. Since low-order schemes avoid these two problems, they have been implemented and compared with the high order schemes in several standard benchmark test cases for interface capture (see [13]). It was observed that second order schemes for LS evolution resulted in similar accuracy as the 5th-order WENO scheme when used in a CLSVOF method. Thus 2nd order schemes were used to evolve LS in this study. The coupling of the F and ϕ equations is effected using the compatibility relationship between them, since both may be used to evaluate the volume fraction in a cell:

$$\overline{F}(x_k^P,t)=\frac{1}{\Omega}\int_{\Omega}H(\overline{\phi}(x_k^P,t))d\Omega$$

Where Ω is the cell volume for the node at x_k^P. To evaluate this numerically it is necessary to generate a description of the interface geometry within the cell at x_k^P from the known values of $\overline{\phi}$ at P and its neighbouring cells. A single interface normal vector is obtained for cell P using $\overline{\phi}$ at P and at a selection of surrounding nodes. The compatibility relation then allows the interface geometry deduced from the $\overline{\phi}$ solution to be adjusted so that it is consistent with the local $\overline{F}_P$ value. $\overline{\phi}$ is then re-initialized to recover the signed distance property. This correction is carried out at several stages of the operator split method, as described in [13], with the adjusted interface used to evaluate the liquid volume flux convection terms in the VOF equation as noted above.

Liquid Velocity Extrapolation Algorithm

The velocity field solution from the governing equations (in 2D u and v), represents the local gas or liquid velocity depending on the local value of $\overline{F}$. It is clearly vital to satisfy continuity and momentum equations in both liquid and gas regions. This introduces difficulties for cells which contain the interface. [6] has already suggested one way to minimise errors associated with such cells by introducing an extrapolated liquid velocity field. A similar but simpler technique is adopted here. A liquid velocity field, denoted by u^L and v^L, is generated within the liquid domain, but also in a small region on the gas phase side of the interface. In the liquid region ($\overline{\phi}>0$), u^L and v^L are simply set equal to u and v; in the gas region ($\overline{\phi}<0$), for a small distance away from the interface, extrapolated liquid velocities u^L and v^L are computed by solving the following equation for a small value of τ (as in the re-initialisation step for $\overline{\phi}$):

$$\frac{\partial u^L}{\partial \tau}+n_k\frac{\partial u^L}{\partial x_k}=0$$

where a forward Euler scheme is used for temporal, and a 1st order upwind scheme for spatial discretisation.

Divergence Free Condition for Extrapolated Liquid Velocity

A volume source term is calculated for cells (i, j) cut by the interface, i.e. where 0<*F*<1:

$$S=u^L_{i-1/2,j}\Delta y_j-u^L_{i+1/2,j}\Delta y_j+v^L_{i,j-1/2}\Delta x_i-v^L_{i,j+1/2}\Delta x_i$$

The liquid velocity field on the gas phase faces of such cells is corrected by an upwind scheme:

$$u^L_{i-1/2,j}=u^L_{i-1/2,j}-a_w\frac{S}{A}\left|n_x\right|_{i-1/2,j}\qquad u^L_{i+1/2,j}=u^L_{i+1/2,j}+a_e\frac{S}{A}\left|n_x\right|_{i+1/2,j}$$

where

$$a_w=\begin{cases}1 & if\ (\phi_{i-1/2,j}<0\ and\ \phi_{i,j}>\phi_{i-1,j})\\ 0 & else\end{cases}\qquad a_e=\begin{cases}1 & if\ (\phi_{i+1/2,j}<0\ and\ \phi_{i,j}>\phi_{i+1,j})\\ 0 & else\end{cases}$$

$$A=a_w\left|n_x\right|_{i-1/2,j}\Delta y_j+a_e\left|n_x\right|_{i+1/2,j}\Delta y_j+a_s\left|n_y\right|_{i,j-1/2}\Delta x_i+a_n\left|n_y\right|_{i,j+1/2}\Delta x_i$$

For more details see [13].

Discretisation of Convection Using Extrapolated Liquid Velocity

In order to reduce momentum discretisation errors for cells containing the two-phase interface, convection terms are calculated using the extrapolated liquid velocity field described above. At large liquid/gas density ratio, the gas has a much smaller inertia than the liquid and flows around liquid structures. Since the shear stress is continuous across the interface and the liquid has a much larger viscosity, the velocity gradient in the liquid phase is much smaller than in the gas phase. Thus, the interface velocity is much closer to the velocity in adjacent liquid cells than that in adjacent gas cells. Therefore, when discretising the momentum equation in cells cut by the interface, large momentum errors can be introduced if the velocity in adjacent gas cells is used to calculation convection terms. The extrapolated liquid velocity in interface containing gas cells provides a more accurate inter-

face velocity. A typical example is shown below for the discretisation of the term $\partial uu/\partial x$ in the u-control-volume $\Omega_{i\text{-}1/2,\,j}$ (for more details see [13]):

$$\int_{\Omega_{i-1/2,j}} \frac{\partial uu}{\partial x}\,\mathrm{d}V = \begin{cases} \left(u^L_{i,j}u^L_{i,j} - u^L_{i-1,j}u^L_{i-1,j}\right)\Delta y_j & if\ \left(\phi_{i-1/2,j} > 0\right) \\ \left(C_{i,j} - C_{i-1,j}\right)\Delta y_j & else \end{cases}$$

$$C_{i,j} = \begin{cases} u^L_{i,j}u^L_{i,j} & if\ \left(\phi_{i-1/2,j} > 0\right) \quad u^L_{i,j} = \dfrac{u^L_{i-1/2,j} + u^L_{i+1/2,j}}{2} \\ u_{i,j}\,u_{i,j} & else \qquad\qquad u_{i,j} = \dfrac{u_{i-1/2,j} + u_{i+1/2,j}}{2} \end{cases}$$

This scheme has been found to stabilise and produce realistic treatment of the interface cells even for high density ratio. For example, [13] shows that a single liquid droplet in an air flow at a Weber No. too low to display any break-up is observed to shatter catastrophically due to interface momentum errors if the extrapolated liquid velocity treatment is omitted. With the treatment described above, it behaves physically correctly across a wide range of Weber Nos., as will be indicated in the Results section.

Treatment of Surface Tension - Ghost Fluid Method

In the current simulation of two-phase flows, the pressure jump across the interface arising from the surface tension is incorporated in the discretisation of the pressure gradient using a Ghost Fluid Method [7]. Ghost and real values of pressure are illustrated in Fig. 2. The pressure gradient at $i-1/2$ is discretised as:

$$\left(\frac{\partial P}{\partial x}\right)_{i-1/2} = \frac{P_i^G - P_{i-1}}{\delta x} = \frac{P_i - [P] - P_{i-1}}{\delta x}$$

$[P]$ is the pressure jump across the interface arising from surface tension. For consistency with the discretisation of the convection term where the x-momentum control volume $\Omega_{i-1/2,\,j}$ is treated as either liquid or gas, in the Poisson equation used to deduce pressure, the density is computed via:

$$\rho_{i-1/2,j} = \begin{cases} \rho_L & if\ \left(\phi_{i-1/2,j} > 0\right) \\ \rho_G & else \end{cases}$$

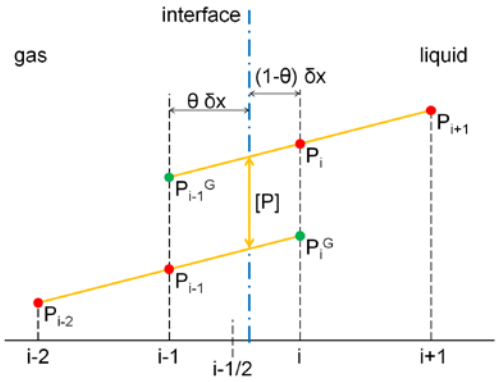

Fig. 2 Ghost fluid method

Results and Discussion

Single Drop Break-up

The break-up of a single liquid droplet of diameter D_0 in a uniform (non-turbulent) air flow at velocity U_G has been studied extensively. Such a flow represents an appropriate first test case for validating the proposed two-phase modelling methodology. Simulations were carried out at three different Weber numbers: 3.4, 13.5, and 100 ($We = \rho_G U_G^2 D_0/\sigma$). The simulated droplet undergoes oscillatory deformation, bag break-up, or sheet-thinning break-up respectively for the three We test cases, agreeing well with experimental observations. 3D views of predicted bag break-up and sheet-thinning break-up at a succession of time instants are shown in Figs 3

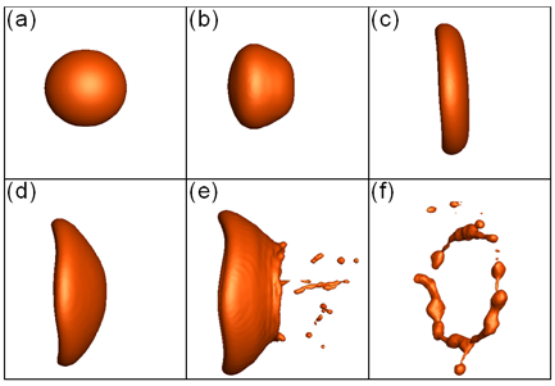

Fig. 3 Predicted bag break-up (We = 13.5) at various times

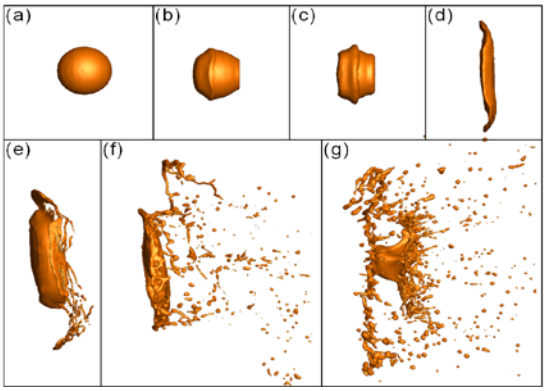

Fig. 4 Predicted sheet-thinning break-up (We = 100) at various times

and 4, which agree well with the shadowgraph and LIF (Laser induced fluorescence) images from [14], showing for example how in bag break-up small droplets are created in the centre and large drops in the bag rim, whereas in sheet-thinning mode small drops are stripped off the disc periphery formed from the flattened initial drop. A

quantitative comparison of variables characterising bag break-up is given in Figs. 5-9 with comparison between experiment and simulation. The droplet break-up process is divided into a deformation stage and a break-up stage. The drop deforms into a liquid disc in the first stage while a bag forms in the disc centre and subsequently disintegrates into ligaments and droplets in the second stage. A characteristic break-up time scale is defined as $t^* = \sqrt{\rho_L/\rho_G}\ D_0/U_G$; the dimensionless time from flow start up is $T = t/t^*$. The initiation time T_{ini} is defined as the elapsed time of the deformation period, which ends at the first sign of bag formation (thinning of the drop central zone); at this moment, the fluid disc reaches its maximum cross-stream dimension D_{max}. T_{ini} and D_{max} are illustrated in Fig. 5. Figs 6 and 7 show that T_{ini} and D_{max} predicted in the current simulations agree closely with experimental values taken from [15]-[18]. Predicted growth of cross-stream diameter in Fig. 8 shows good

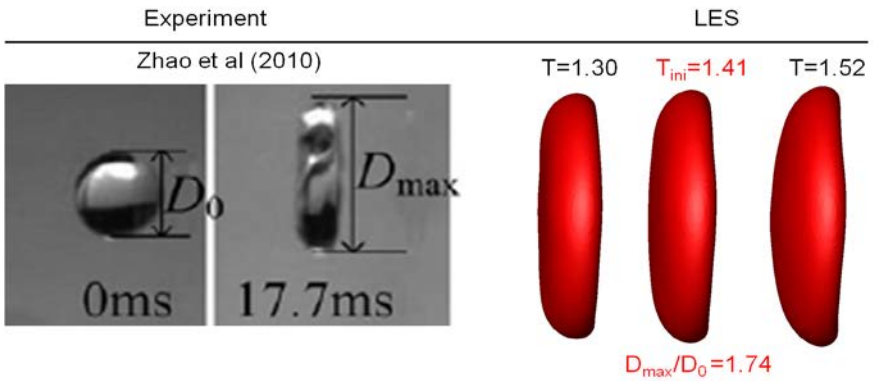

Fig. 5 Initiation time T_{ini} and maximum cross-stream diameter D_{max} (air flow from left to right.)

agreement with data. In Fig. 9 the predicted drag coefficient increases from ~0.45 to ~1.2 as the drop deforms from a sphere to a disc, agreeing well with the measurements of [16]. Fluctuations in drag arise from the unsteadiness of large eddies in the drop wake. C_D was extracted using predicted drop centre of mass acceleration.

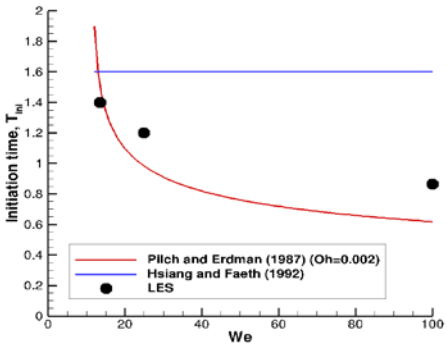

Fig. 6 Comparison of T_{ini} LES/Expts.

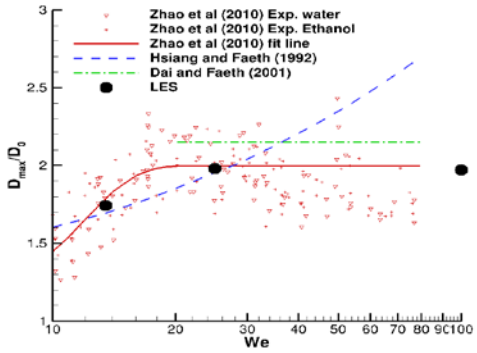

Fig. 7 Comparison of D_{max} LES/Expts

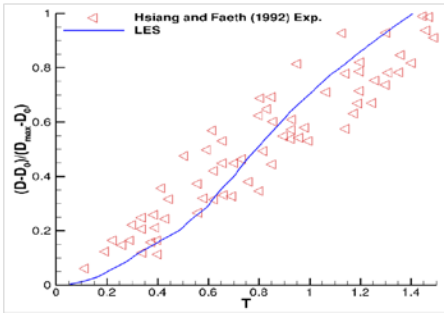

Fig. 8 Growth of droplet diameter D

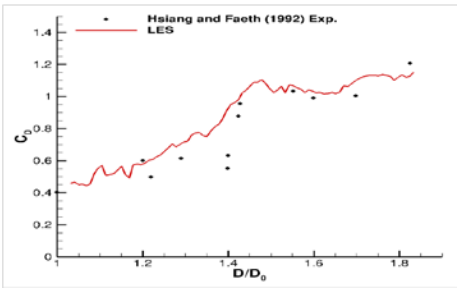

Fig. 9 Instantaneous drag coefficient C_D

The sensitivity of drop size distribution to mesh size is often queried but rarely explored. Figs. 10 and 11 present results obtained for a bag break-up case. Four grids were used with the finest having cell size Δ_0 = 0.06mm as in Figs. 5-9. Coarser meshes were used with $\Delta_1 = \sqrt{2}\,\Delta_0$, $\Delta_2 = 2\Delta_0$, $\Delta_3 = 4\Delta_0$. Fig. 10 shows predicted temporal growth of drop cross-stream dimension D_c. On the coarsest mesh, no drop break-up was observed, but on the 3 finer meshes, drop break-up does occur and convergence of growth rate is observed. The predicted initiation

time is the same for Δ_2, Δ_1, and Δ_0 at T=1.36. Bag bursting also starts at the same time (within 5%) at T=2.0 Fig. 11 shows break-up of the bag rim (Plateau-Rayleigh instability) and the resulting drop fragments on the two finer meshes. With mesh Δ_2, only 4 nodes and 4 drops were formed; with the two finer meshes, the resulting droplet number shows convergence (8 with Δ_1 and 10 with Δ_0). Break-up is completed at T=3.84 on meshes Δ_2, Δ_1, Δ_0.

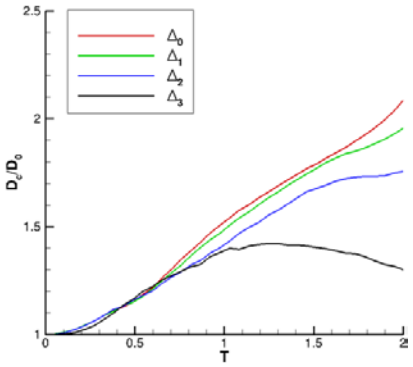

Fig. 10 D_c growth - mesh effects

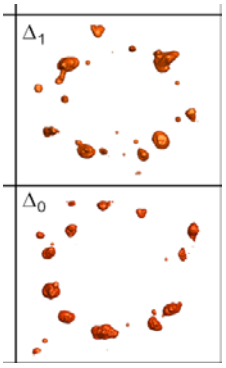

Fig. 11 Bag rim break-up - mesh effects

Liquid Jet Atomisation in Coaxial Air Flow

The atomisation of an axisymmetric water jet in co-axial air flow was studied in [19]. The liquid core length (jet break-up length) L_c was defined as the location where the continuity of the liquid jet is interrupted, an important parameter for atomisation performance. Measurements of L_c via the shadowgraph technique can contain significant error due to obscuration by atomised droplets of the jet core. A novel technique based on liquid column laser induced fluorescence (LIF), was used in [19] to measure L_c, providing more accurate detection of the liquid jet structure. This L_c data is used here to validate LES predictions of liquid jet primary break-up. Fig. 12 presents (a) the atomiser geometry, (b) a shadowgraph of the liquid [19], and (c), (d) two instantaneous images of predicted break-up with liquid and air velocities 4m/s and 47m/s. When a uniform, zero turbulence, outflow from nozzle exit is used - (c) - the predicted liquid core is much longer than measured, and no droplets and ligaments are observed unlike in the experiment. To specify a more realistic nozzle exit condition in the LES (corresponding to the high Re nature of the flow), a Rescaling-Recycling Method (R^2M) [20] has been introduced for LES inlet condition generation. In R^2M, two extra Inlet Condition (IC) domains are created upstream of nozzle inlet for single-phase LES of the gas and liquid inflows. The unsteady flows generated in the IC domains are used as the inflows to the Main Simulation (MS) domain where jet flow/break-up is resolved. By providing 'target' statistical turbulence data as input to the R^2M simulations in the IC domains, unsteady but spatially and temporally correlated inlet conditions, which possess the same statistical features as specified in the target data (time-averaged profiles of mean velocity and turbulence normal stresses) may be provided to the MS domain LES calculation. The target data were generated in the present work from RANS CFD (Reynolds Stress Transport turbulence model) of the internal atomiser flow. The R^2M generates unsteady inlet conditions, which feature realistic and self-consistent turbulent eddy structures, as demonstrated in Fig. 13. Turbulent eddy structures developed in the nozzle internal flow are convected downstream into the MS domain as the air/water flows exit the nozzle. These turbulent eddies are sufficiently energetic that they disturb the two-phase interface immediately after nozzle, so that the smooth interface seen in the uniform zero turbulence case (Fig. 12c) is now much shorter (Fig.12d). Fig. 14 shows a close up of the near nozzle region and the different behaviour of the interface when nozzle exit turbulence is present. If the initial interface perturbations are captured correctly, the predicted erosion of the liquid core under strong turbulence and aerodynamic forces agrees well with the experiment. Fig. 15 presents predicted break-up lengths at different air velocities and constant water velocity. Close agreement with measured data when using R^2M is seen over the whole We No. range studied. At low We No. the initial interface instability due to turbulent eddies convected downstream from the nozzle plays an important role in jet core disintegration; at higher We (~1000), the strong aerodynamic forces dominate the primary break-up process, so the difference between the two calculations is much less.

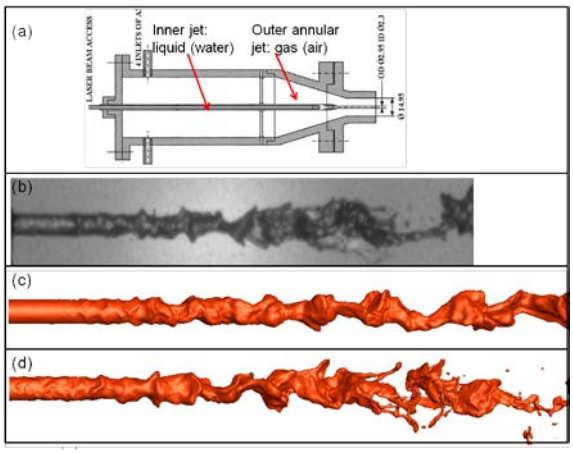

Fig. 12 Coaxial jet break-up;

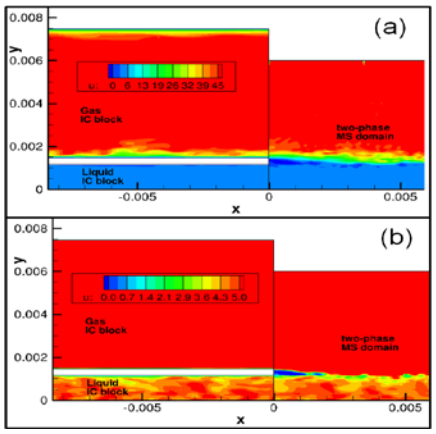

Fig. 13 LES predicted u-contours, showing turbulent structures in: (a) air; (b) liquid

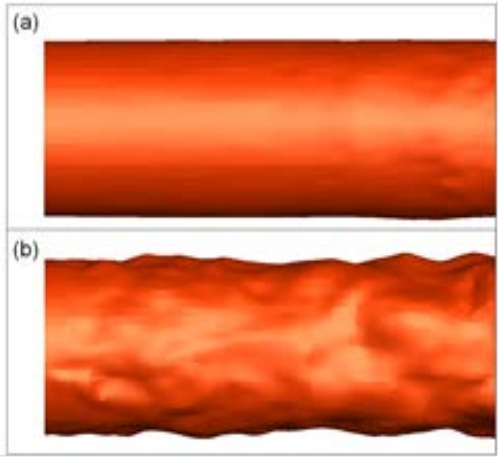

Fig. 14 LES predicted interface near nozzle exit (a) uniform laminar inflow; (b) turbulent inflow

Summary and Conclusions

An LES algorithm for two-phase flows has been developed and applied in the present paper. Two test cases were presented to demonstrate that the proposed method is accurate and robust, even at high liquid/gas density ratio. The break-up of a single drop shows that the effects of aerodynamic forces on the drop are correctly captured by the present LES method, resulting in a break-up process in good agreement with experiments. The simulations of a liquid jet in a coaxial air flow show that the predicted liquid core length agrees well with experiment, indicating the first stage of primary break-up can be well reproduced. This test case illustrated the importance of an accurate method for representing turbulence structures present in inflow conditions for LES. These results are now being extended to a liquid jet in a turbulent air cross-flow.

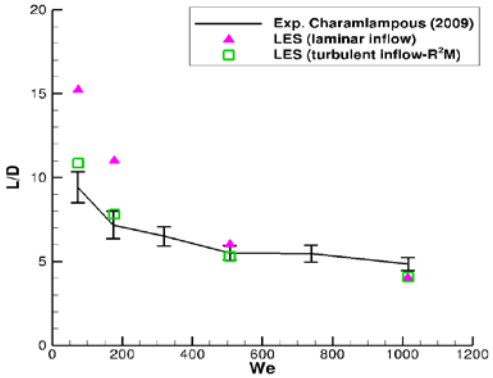

Fig. 15 Liquid core length at different We.

Acknowledgements

Work carried out in the Loughborough UTC in Combustion System Aerothermal Processes. Financial support from EPSRC (SAMULET project and Dorothy Hodgkin Award for the first author) is gratefully acknowledged.

References

[1] Herrmann M., ASME Journal of Engineering for Gas Turbines and Power 132:061506, 2010.
[2] Lebas R., Ménard T., Beau P. A., Berlemont A., & Demoulin F. X., Int. J. of Multi. Flow 35:247-260, 2009.
[3] Desjardins O., Moureau V., and Pitsch H., Journal of Computational Physics 227:8395-8416, 2008.
[4] Tomar G., Fuster D., Zaleski S., and Popinet S., Computers & Fluids 39-10:1864-1874, 2010.
[5] Li X., Arienti M., Soteriou M., C., & Sussman, M., AIAA2010-0210, 48th Aero. Sci., Orlando, USA, 2010.
[6] Sussman M., Smith K., Hussaini M. Y., Ohta M., & Zhi-Wei R., J. of Comp. Phys., 221-2: 469-505, 2007.
[7] Fedkiw R., Aslam T., Merriman B., and Osher S., Journal of Computational Physics 152:457-492, 1999.
[8] Hermann M. & Gorokhovski M., ICLASS 2009 Conf., Vail, USA, July 2009.
[9] Gorokhovski M. & Hermann M., Ann. Rev. of Fluid Mech., 40:342-366, 2008.
[10] Sussman, M., and Puckett, E. G., Journal of Comp. Phys., 162:301-337, 2000.
[11] Park S. W. and Kim S. and Lee C. S., International Journal of Multiphase Flow, 32-7:807-822, 2006.
[12] Ren Y. X., Liu M. E., and Zhang H.-X., Journal of Computational Physics, 2:365-386, 2003.
[13] Xiao F., *Large Eddy Simulation of Liquid Jet Primary Break-up*, PhD thesis, Loughborough Univ., 2012.
[14] Theofanous T. G., Li G. J., Dinh T. N., and Chang C.-H., Journal of Fluid Mechanics, 593:131-170, 2007.
[15] Zhao H., Liu H.-F., Li W.-F., and Xu J.-L., Physics of Fluids, 22:11410, 2010.
[16] Hsiang L-P., and Faeth G. M., International Journal of Multiphase Flow, 18:635-652, 1992.
[17] Pilch M. and Erdman C. A., International Journal of Multiphase Flow 13:741-757, 1987.
[18] Dai Z., Faeth G. M., International Journal of Multiphase Flow 27:217-236, 2001.
[19] Charalampous G., Hardalupas Y. & Taylor A. M., AIAA Journal 47:2605-2615, 2009.
[20] Xiao F., Dianat M., and McGuirk J. J., Proc. 8th Int Symp. on ETMM, Marseille, France, June, 2010.